

07.2;07.3

Solar-blind Schottky photodiodes based on the AlGa_N:Si/AlN heterostructures grown by plasma-activated molecular beam epitaxy

© A.N. Semenov¹, D.V. Nechaev¹, D.S. Burenina¹, I.P. Smirnova¹, Yu.M. Zadiranov¹, M.M. Kulagina¹, S.I. Troshkov¹, N.M. Shmidt¹, A.I. Lihachev¹, V.S. Kalinovskiy¹, E.V. Kontrosh¹, K.K. Prudchenko¹, A.V. Nahornii², E.V. Lutsenko², V.N. Jmerik¹

¹Ioffe Institute, St. Petersburg, Russia

²Stepanov Institute of Physics, Belarusian Academy of Sciences, Minsk, Belarus

E-mail: semenov@beam.ioffe.ru

Received April 24, 2024

Revised June 24, 2024

Accepted June 25, 2024

The article describes solar-blind Schottky photodiodes based on the AlN/Al_{0.7}Ga_{0.3}N/Al_{0.55}Ga_{0.45}N heterostructures grown by plasma-activated molecular beam epitaxy on *c*-sapphire substrates with various AlN buffer layers. X-ray diffraction analysis and chemical surface etching were used to estimate the density of threading dislocations that affect leakage currents and spectral sensitivity of photodiodes. Optimization of the photodiode design and Ti/Al/Ti/Au contact layer made it possible to achieve photosensitivity of 51 mA/W in the solar-blind range ($\lambda < 290$ nm) in the photovoltaic mode.

Keywords: plasma-activated molecular beam epitaxy, solar-blind Schottky photodiodes, AlGa_N, threading dislocations.

DOI: 10.61011/TPL.2024.10.60120.19972

Solar-blind ultraviolet (UV) photodetectors with sensitivity at the wavelengths below 290 nm are desirable in many popular applications, such as detection of UV radiation in spectroscopy systems and from various atmospheric UV sources, as well as in the field of highenergy physics for detecting the fast component of radiation from BaF₂ crystals [1]. Solar-blind photodetectors comprise AlGa_N layers with a high content of aluminum (> 40 mol.%) for which the *p*-type conductivity can hardly be achieved [2]. Therefore, photodiodes with a Schottky barrier which, unlike *p-i-n* photodiodes, comprise only *n*-doped layers, represent one of the most promising types of solar-blind photodetectors [3]. Output characteristics of photodetectors are largely governed by their leakage currents whose level in the AlGa_N photodiodes may be high due to high density of threading dislocations (> 10⁹ cm⁻²) arising during epitaxial growth of heterostructures on *c*-sapphire or crystalline-silicon substrates [4]. Therefore, quite a lot of attention is paid to developing techniques for suppressing the nucleation of these dislocations and limiting their propagation in the growth direction [5].

This article considers Schottky photodiodes based on the *n*-AlGa_N:Si/AlN heterostructures grown by plasma-activated molecular beam epitaxy (PA MBE) on vicinal *c*-sapphire substrates (0.2° misorientation from the *M* plane) with templates and AlN buffer layers. The templates were grown by both PA MBE and metal-organic vapor phase epitaxy (MOVPE); the methods provided different threading dislocation densities and, hence, different leakage currents and spectral sensitivities of Schottky photodiodes.

The Schottky diode structure is shown schematically in Fig. 1, *a*; parameters of the layers are listed in the Table. Specific features of PA MBE growth of the AlN nucleation and buffer layers are described in detail in [6]. Upper AlGa_N:Si layers were grown at the substrate temperature $T_S = 700^\circ\text{C}$ and differed in thickness, Al content (55 and 70 mol.%) and doping level (see the Table). Nominally, doping levels of layers with equal aluminum contents were identical; the difference in electron concentrations (see the Table) was apparently caused by different conditions for Si embedding due to differences in the buffer layers. The AlGa_N layers were grown under metalenriched conditions at flow ratio (Al+Ga)/N₂=1.8 with periodic growth interruptions necessary for evaporating excess metal (Ga) [7]. After reactive ion-plasma etching of mesa structures, an *n*-contact Ti (25 nm)/Al (80 nm)/Ti (60 nm)/Au (100 nm) was deposited by e-beam sputtering on the lower *n*-doped Al_{0.7}Ga_{0.3}N:Si layer; the contact was annealed at 900°C for 60 s, which ensured the ohmic contact resistance of $\sim 8 \Omega \cdot \text{mm}$ [8]. Active regions were slightly doped *n*-Al_{0.55}Ga_{0.45}N:Si layers 200 nm thick; Ni (30 nm)/Au (100 nm) layers to be used as contacts were deposited by sputtering onto their surface without firing. The diameter of these contacts (photodiode active regions) varied from 30 to 400 μm.

All the structures were examined by using scanning electron microscopes (SEM) JSM 7001F (JEOL, Japan) and CamScan 4-88-DV-100 (UK). Concentrations of threading dislocations with screw and edge components whose values are listed in the Table were determined based on measurements of, respectively, half-widths (ω) of symmetric

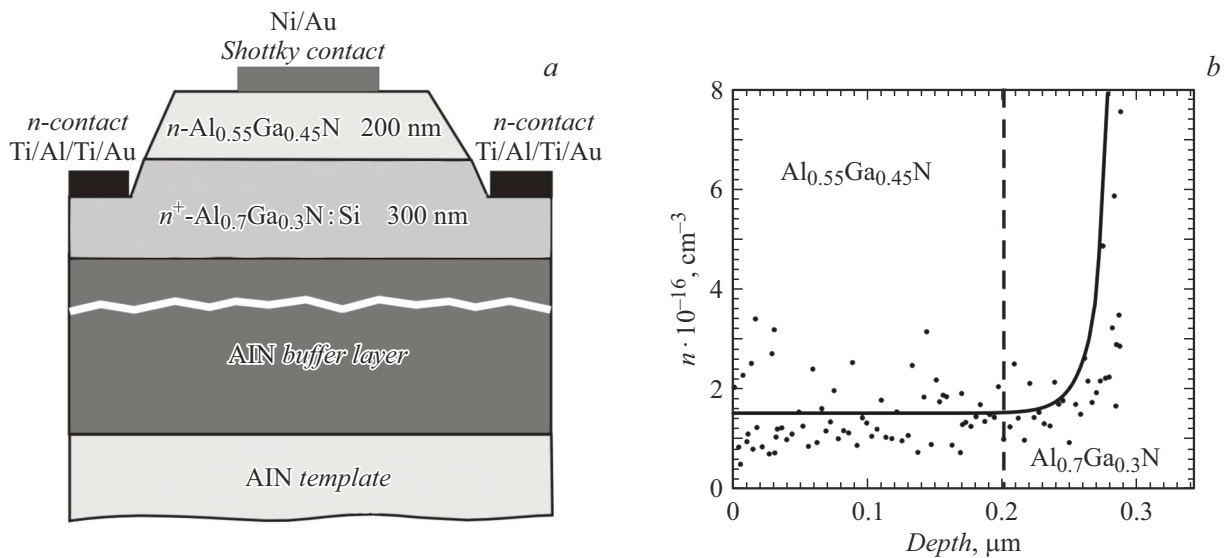


Figure 1. Schematic representation of the Schottky diode structure (a) and variation in the electron concentration along the structure depth (b).

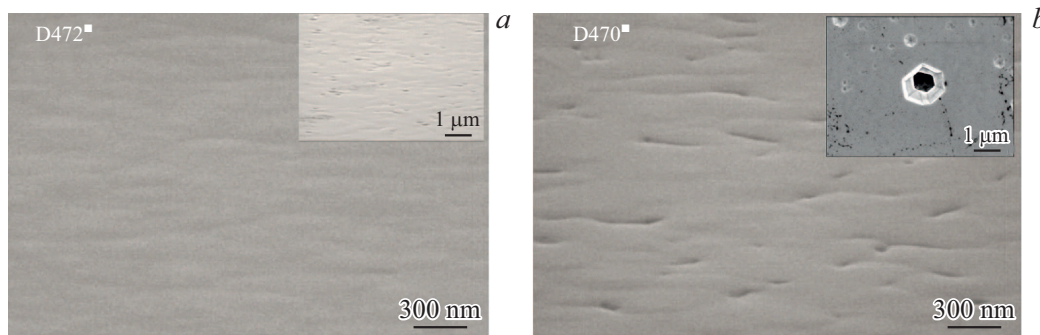


Figure 2. Surface SEM images of structures grown on the AlN(PA MBE) buffer layer (structures A and B) (a) and AlN(MOVPE) buffer layer (structure C) (b). The insets present images after etching in H_3PO_4 .

(0002) and obliquely symmetric (10-15) X-ray diffraction reflections [9]. To estimate those concentrations, standard formula $N = \omega^2 / (4.35b^2)$ [10] was used, where b is the Burgers vector of either a screw dislocation or of an edge one. In addition, concentrations of threading dislocations were measured by the metallographic method involving chemical etching of heterostructures either in H_3PO_4 at $160^\circ C$ for 15 s or in the 20% KOH solution at $90^\circ C$ for 5 min.

Charge carrier concentrations in the AlGaN layers were determined by using a mercury probe on contactless test structures; for the $Al_{0.55}Ga_{0.45}N$ active region, the $C-V$ method was additionally used on structures with contacts (Fig. 1, b). The photodiodes sensitivity spectra were measured on the structures illuminated by a tunable UV radiation source from the side of substrate at zero external voltage (photovoltaic mode).

Fig. 2 presents SEM images of the surfaces of Schottky photodiode epitaxial heterostructures, which exhibit a satisfactory planar morphology. Though the heterostructure

grown on the AlN(MOVPE) template had surface features similar to those of the heterostructures grown on AlN(PA MBE) templates, their local relief inhomogeneities (dips) (Fig. 2, b) were greater (Fig. 2, a).

The Table presents the estimates of threading dislocation densities obtained from the data of X-ray diffraction analysis, which show that the edge dislocation densities in the AlN(MOVPE) template are almost an order of magnitude lower than those in the AlN(PA MBE) template. Densities of screw dislocations differ only twice.

Despite the high dislocation density, samples with AlN(PA MBE) templates (samples A and B) exhibited no signs of surface etching in orthophosphoric acid. When using a 20% KOH solution having a higher etching rate, noticeable etching was observed over the entire surface of the sample. However, etching selectivity was insufficient, which prevented accurate calculation of the etch pits (defects) density. Structure C grown on the AlN(MOVPE) template was the only one where the metallographic method in etchant H_3PO_4 allowed identifying screw and edge

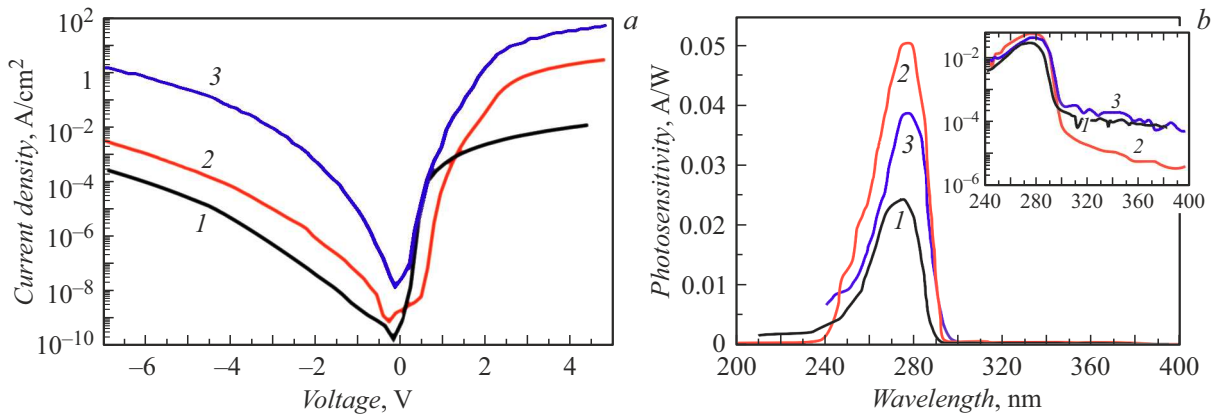


Figure 3. I-V characteristics of the Schottky photodiodes under study (*a*) and their spectral characteristics (*b*). 1 — structure A (photosensitivity of 24 mA/W), 2 — structure B (photosensitivity of 51 mA/W), 3 — structure C (photosensitivity of 40 mA/W). The inset presents the logarithmic dependence of spectral photosensitivity.

Main parameters of the Schottky diodes

Structure	Buffer	Active region		Wide-gap window (<i>n</i> -contact layer)		Density of dislocation, cm ⁻²	
		<i>x</i>	<i>n</i> , cm ⁻³	<i>x</i>	<i>n</i> , cm ⁻³	Edge	Screw
A	1 μm, PA MBE	0.55	~ 5 · 10 ¹⁶	0.7	> 5 · 10 ¹⁷	~ 1 · 10 ¹⁰	1 · 10 ⁹
B	2 μm, PA MBE	0.55	~ 1 · 10 ¹⁶	0.7	> 1 · 10 ¹⁷	7 · 10 ⁹	6 · 10 ⁸
C	2 μm, MOVPE	0.55	~ 1 · 10 ¹⁶	0.7	> 1 · 10 ¹⁷	1 · 10 ⁹	5 · 10 ⁸

dislocations (see the inset to Fig. 2, *b*). Screw and edge threading dislocations manifested themselves as etch pits having the shape of truncated and pointed inverse pyramids, respectively (inset to Fig. 2, *b*). Estimates of dislocation densities coincided with those obtained by X-ray diffraction.

It is known that, in the case of the AlN(MOVPE) templates, threading dislocations have an open-core structure, which leads to formation of V-shaped defects at the places where dislocations reach the surface; the defect sizes increase during chemical etching, which results in formation of the observed etch pits [11]. Surface of AlGa_N layers grown on the AlN(PA MBE) templates is of a different character, which is associated with stoichiometric conditions more metal-enriched than in the MOVPE mode when nitrogen-enriched conditions are typically used. Apparently, this is the main reason for the formation in this case of full-core threading dislocations. Previously, dislocations with such a structure were found in [12] by transmission electron microscopy. As a result, planarity of the AlGa_N layers grown on the AlN(PA MBE) templates does not get disrupted at the places where threading dislocations emerge to the surface. Moreover, those places turn out to be chemically inert to etching in phosphoric acid.

Fig. 3 presents the dark current-voltage (I-V) characteristics and spectral characteristics for various types of Schottky photodiode structures. As Fig. 3, *a* shows, scatter of the dark current density on the structures I-V curve reverse branch exceeds four orders of magnitude. Contrary to expectations,

the lowest dark current densities (50 nA/cm² at -2 V) are exhibited by structure A having the maximal dislocation concentration. An increase in the buffer layer thickness and decrease in the dislocation density in structure B did not lead to a decrease in the dark current density. Finally, structure C exhibiting the minimal threading dislocation concentration is characterized by the maximal density of dark current that is almost two orders of magnitude higher than in other structures. This increase in current is most likely caused by high defectiveness of grain boundaries in the AlGa_N layers grown on the AlN(MOVPE) templates, which is clearly seen in the surface SEM image (Fig. 2, *b*).

These results demonstrate the absence of a clear correlation between photodiode dark current densities and threading dislocations in the structure. This evidences for a complex nature of the conduction channels formation in AlGa_N with threading dislocations and of their effect on the dark current densities and contact resistances in Schottky diodes. For the purpose of further investigation of this relationship, spatial maps of leakage current will be measured by using atomic force microscopy.

Fig. 3, *b* shows the Schottky diode spectral characteristics at zero bias (the inset presents logarithmic spectral characteristics). All the three diodes demonstrate maximum sensitivity at the wavelength of 272–274 nm which corresponds to the bandgap of the Al_{0.55}Ga_{0.45}N active layer.

The lowest photosensitivity (24 mA/W) was exhibited by structure A despite the minimal dark current densities.

Apparently, high dislocation density in this structure resulted in a decrease in the diffusion length of photogenerated charge carriers, which reduced the photodiode sensitivity. The maximal photosensitivity (51 mA/W) was measured in structure *B*; this was promoted by a relatively low dislocation density. Sensitivity of structure *C* appeared to be 40 mA/W.

Thus, this article demonstrates the possibility of creating solar-blind Schottky photodiodes based on the Al_{0.55}Ga_{0.45}N:Si/Al_{0.7}Ga_{0.3}N:Si heterojunction with high spectral sensitivity (51 mA/W) at the wavelength of ~ 270 nm. In addition, the study has demonstrated that the standard metallographic method (etching in H₃PO₄) differently reveals the presence of threading dislocations in the AlN/c-Al₂O₃ templates grown by different methods: MOVPE and PA MBE under metal-enriched conditions. In the first case application of the method encounters no problems, but in the second one the template surfaces are chemically inert despite high density of threading dislocations in them.

Acknowledgements

Electron microscopy investigations were partially performed using the facilities of Federal Collective Use Center „Materials Science and Diagnostics in Advanced Technologies“.

Funding

The study was supported by the RF Ministry of Science and Higher Education (contract № 075-15-2022-1224 Bio-Svet).

Conflict of interests

The authors declare that they have no conflict of interests.

References

- [1] W. Fang, Q. Li, J. Li, Y. Li, Q. Zhang, R. Chen, M. Wang, F. Yun, T. Wang, *Crystals*, **13** (6), 915 (2023). DOI: 10.3390/cryst13060915
- [2] G. Namkoong, E. Trybus, K.K. Lee, M. Moseley, W.A. Doolittle, D.C. Look, *Appl. Phys. Lett.*, **93** (17), 172112 (2008). DOI: 10.1063/1.3005640
- [3] N. Biyikli, O. Aytur, I. Kimukin, T. Tut, E. Ozbay, *Appl. Phys. Lett.*, **81** (17), 3272 (2002). DOI: 10.1063/1.1516856
- [4] L. Gautam, J. Lee, G. Brown, M. Razeghi, *IEEE J. Quantum Electron.*, **58** (3), 4000205 (2022). DOI: 10.1109/JQE.2022.3154475
- [5] S. Pharkphoumy, V. Janardhanam, T.-H. Jang, K.-H. Shim, C.-J. Choi, *Electronics*, **12** (4), 1049 (2023). DOI: 10.3390/electronics12041049
- [6] D.V. Nechaev, P.A. Aseev, V.N. Jmerik, P.N. Brunkov, Y.V. Kuznetsova, A.A. Sitnikova, V.V. Ratnikov, S.V. Ivanov, *J. Cryst. Growth*, **378**, 319 (2013). DOI: 10.1016/j.jcrysgro.2012.12.080
- [7] D.V. Nechaev, P.N. Brunkov, S.I. Troshkov, V.N. Jmerik, S.V. Ivanov, *J. Cryst. Growth*, **425**, 9 (2015). DOI: 10.1016/j.jcrysgro.2015.03.055
- [8] A.N. Semenov, D.V. Nechaev, D.S. Berezina, Yu.A. Guseva, M.M. Kulagina, I.P. Smirnova, Yu.M. Zadiranov, S.I. Troshkov, N.M. Shmidt, *St. Petersburg Polytech. University J. Physics and Mathematic*, **16** (1.3), 182 (2023). DOI: 10.18721/JPM.161.331
- [9] D. Hull, D.J. Bacon, *Introduction to dislocations*, 5th ed. (Elsevier, 2011).
- [10] T. Metzger, R. Höpler, E. Born, O. Ambacher, M. Stutzmann, R. Stömmer, M. Schuster, H. Göbel, S. Christiansen, M. Albrecht, H.P. Strunk, *Phil. Mag. A*, **77** (4), 1013 (1998). DOI: 10.1080/01418619808221225
- [11] M.W. Moseley, A.A. Allerman, M.H. Crawford, J.J. Wierer, M.L. Smith, A.M. Armstrong, *J. Appl. Phys.*, **117** (9), 095301 (2015). DOI: 10.1063/1.4908543
- [12] Z. Liliental-Weber, D. Zakharov, J. Jasinski, M.A. O’Keefe, H. Morkoc, *Microsc. Microanal.*, **10** (1), 47 (2004). DOI: 10.1017/S1431927604040309

Translated by EgoTranslating